

On the diffusion of water in silicalite-1: MD simulations using ab initio fitted potential and PFG NMR measurements

C. Bussai^{a,b}, S. Vasenkov^b, H. Liu^b, W. Böhlmann^b, S. Fritzsche^{b,*},
S. Hannongbua^a, R. Haberlandt^b, J. Kärger^b

^a Department of Chemistry, Faculty of Science, Chulalongkorn University, Bangkok 10330, Thailand

^b Faculty of Physics and Geoscience, University of Leipzig, Linnéstreet 5, 04103 Leipzig, Germany

Received 10 October 2001; received in revised form 23 January 2002; accepted 23 January 2002

Abstract

Molecular dynamics simulations of water diffusion in silicalite-1 are reported. The simulations are carried out using an ab initio fitted silicalite-1–water potential based on quantum chemical calculations. In addition, preliminary results of pulsed field gradient (PFG) NMR diffusion measurements of water and small alkane molecules in silicalite-1 samples are presented. Pre-adsorption of water in silicalite-1 samples was found to change the intra-crystalline diffusivities of small alkane molecules in silicalite-1. This is interpreted as an indirect evidence that under our experimental conditions water molecules occupy a significant part of the silicalite-1 channel system. The preliminary results of the PFG NMR diffusion measurements of water in silicalite-1 samples are discussed in terms of the contributions of extra- and intra-crystalline water to the measured signals. An order-of-magnitude agreement between the measured and the simulated intra-crystalline diffusivities of water in silicalite-1 is obtained. © 2002 Elsevier Science B.V. All rights reserved.

Keywords: Diffusion coefficient; Silicalite-1; Water; Ab initio fitted potential; Molecular dynamics; PFG NMR

1. Introduction

Zeolites have found applications in various fields of industry as catalysts and molecular sieves [1–3]. Unlike conventional, high-aluminum-content zeolites, silicalite-1 possesses a channel system, which can be regarded as cation-free. Silicalite-1 is widely used to separate paraffin or aromatics from water or other polar solvents as well as to sieve the molecules having different shapes [4–6]. Owing to low aluminum content, the affinity of this zeolite-to-water is weak. Earlier measurement of water diffusion in pentasil zeolites have been published [7], but there are experimental indications that water molecules can, at the best, occupy

only a part of the available pore volume of silicalite-1 crystals [8]. The presence of defect sites, such as hydroxyl groups on the surface of the silicalite-1 channels, may significantly affect the adsorption of water molecules [8].

In this paper, we report the results of molecular dynamics simulations of water diffusion in silicalite-1. We also present here the first, preliminary results of pulsed field gradient (PFG) NMR measurements of water diffusion in samples of silicalite-1. In addition, PFG NMR diffusion measurements of ethane, propane and *n*-butane in water-free samples of silicalite-1 and in silicalite-1 samples with pre-adsorbed water are reported and discussed. The latter measurements were performed in order to study the influence of pre-adsorbed water on the diffusion of alkane

* Corresponding author.

molecules in silicalite-1. An experimental detection of such an influence can be regarded as an indirect evidence that water molecules occupy a significant part of the silicalite-1 channel system.

2. Molecular dynamics simulations

2.1. Methodology and the used *ab initio* fitted potential

To obtain the self-diffusion coefficient by means of a theoretical approach, molecular dynamics simulations [9,10] have been performed at 298 and 393 K. Simulations have been carried out with a time step of 0.5 fs with a MD box consisting of two silicalite-1 unit cells. The system has been examined at a concentration of two water molecules per intersection corresponding to 16 water molecules per MD box and experimentally equivalent to water–silicalite-1 mass ratio (w/s) of 24 mg g⁻¹. Before starting evaluations each system was thermalized for 0.5 ps. Some trial calculations with longer thermalization showed no difference in the diffusion coefficients within the range of fluctuations. The evaluation part of the MD runs corresponded to trajectory lengths of 10 ns. There was no thermalization during the evaluation part of the run. Periodic boundary conditions have been applied. The silicalite-1 crystal structure used in this study is characterized by the two types of channels and belongs to the “Pnma” symmetry group. The crystallographic cell [11] (Si₉₆O₁₉₂) contains 288 atoms with lattice parameters $a = 20.07 \text{ \AA}$, $b = 19.92 \text{ \AA}$ and $c = 13.42 \text{ \AA}$. The potential proposed by Bopp et al. [12] was employed to describe water–water interactions, with the stabilization energy of $-6.1 \text{ kcal mol}^{-1}$ at O–O distance of 2.86 Å. A recently developed potential:

$$\Delta E(w, s) = \sum_i^3 \sum_j^{288} \left\{ \frac{A_{ij}^{ab}}{r_{ij}^6} + \frac{B_{ij}^{ab}}{r_{ij}^{12}} + \frac{C_{ij}^{ab}}{r_{ij}^3} + \frac{q_i q_j}{r_{ij}} \right\}, \quad (1)$$

was used to represent the silicalite-1–water interactions. A , B and C parameters are obtained from 1032 water-framework interaction energies calculated quantum mechanically. Here, the framework is

represented by the three fragments taken from the sinusoidal, straight and intersection channels and water coordinates were generated inside those fragments. Eq. (1) contains 24 fitting parameters and six different atomic net charges, distinguishing interactions between Si and O atoms of silicalite in different channels and O and H atoms of water molecule. The optimal water-framework interaction energy is $-7.0 \text{ kcal mol}^{-1}$. This energy is achieved when the water molecule resides at the center of the interaction channel [13]. A detailed description of the method used for the potential calculations from *ab initio* data is given in [13].

In the present simulations, the lattice was kept fixed while the water molecules are flexible. This approximation is in agreement with the findings observed for methane in silicalite-1 [14], where the effect of host–guest flexibility is already sufficiently accounted for if only the molecules are considered to be flexible while the lattice is kept rigid.

In [15,16], it has been shown that the use of Ewald summations for the Coulomb interactions can be avoided for the treatment of charged particles in zeolites [15] if the sum of all charges in the MD box is zero. Especially in the paper of Wolf et al. [16] it has been shown in detail that this approximation works surprisingly well. Taking into account that Ewald summation may produce the artifacts due to an artificial periodicity of long-range forces arising from distant water atoms, in the present paper we use the approximation proposed by Wolf et al. [16]. This approximation essentially means the use of shifted forces.

In this work, the silanol group free lattice was used. The elucidation of the potentially strong influence of these groups on water diffusion and adsorption in real silicalite-1 crystals remains to be the subject of future research.

2.2. Molecular dynamics results

The self-diffusion coefficients are calculated from the particle displacements. In [20–22], the process of self-diffusion was quite generally related to the moments of the propagator [20]. The propagator $P(\mathbf{r}, \mathbf{r}_0, t)$ represents the probability density to find a particle at position \mathbf{r} at time t when it was at \mathbf{r}_0 at time $t = 0$.

The n th moment of the propagator is defined by the relation [20]:

$$\langle |\mathbf{r} - \mathbf{r}_0|^n \rangle = \int |\mathbf{r} - \mathbf{r}_0|^n P(\mathbf{r}, \mathbf{r}_0, t) d\mathbf{r}, \quad (2)$$

$P(\mathbf{r}, \mathbf{r}_0, t)$ is the solution of the diffusion equation for the initial concentration $C(\mathbf{r}, t = 0) = \delta(\mathbf{r} - \mathbf{r}_0)$. In the case of isotropic diffusion and a homogeneous system the propagator results to be:

$$P(\mathbf{r}, \mathbf{r}_0, t) = (4\pi Dt)^{-3/2} \exp\left\{-\frac{(\mathbf{r} - \mathbf{r}_0)^2}{4Dt}\right\}. \quad (3)$$

Although zeolites are not homogeneous the propagator can be represented in this way if the displacements exceed the size of the inhomogeneities [21]. Then $P(\mathbf{r}, \mathbf{r}_0, t)$ depends only on the difference $|\mathbf{r} - \mathbf{r}_0|$. For shorter times this is not true. As the transition time to the Gaussian behavior and the final D values were the quantities of main interest in the present paper an averaging over \mathbf{r}_0 has been carried out. The resulting propagator depends only upon $|\mathbf{r} - \mathbf{r}_0|$ for all times. But, it attains the shape shown in Eq. (3) (or its equivalents for the different components of the diffusion tensor in the anisotropic case, as shown below) only for sufficiently long times.

The first four moments can be calculated from Eqs. (2) and (3) in the case of normal diffusion as:

$$\langle |\mathbf{r} - \mathbf{r}_0| \rangle = 4\sqrt{\frac{Dt}{\pi}}, \quad (4)$$

$$\langle |\mathbf{r} - \mathbf{r}_0|^2 \rangle = 6Dt, \quad (5)$$

$$\langle |\mathbf{r} - \mathbf{r}_0|^3 \rangle = \frac{32}{\sqrt{\pi}}(Dt)^{3/2}, \quad (6)$$

$$\langle |\mathbf{r} - \mathbf{r}_0|^4 \rangle = 60(Dt)^2. \quad (7)$$

In the anisotropic system, the corresponding equations for each direction are [14]:

$$\langle |l - l_0| \rangle = 2\sqrt{\frac{D_l t}{\pi}}, \quad (8)$$

$$\langle |l - l_0|^2 \rangle = 2D_l t, \quad (9)$$

$$\langle |l - l_0|^3 \rangle = \frac{8}{\sqrt{\pi}}(D_l t)^{3/2}, \quad (10)$$

$$\langle |l - l_0|^4 \rangle = 12(D_l t)^2, \quad (11)$$

where l is x , y or z , respectively. The D values estimated from these four moments must synchronize each other in the case of normal diffusion for t values that are larger than the decay time of the velocity auto-correlation function. The elements of the diffusion tensor, corresponding to the x -, y - and z -axis are calculated from Eqs. (8)–(11). In this case, the diffusivity D is one-third of the trace of the diffusion tensor:

$$D = \frac{1}{3}(D_x + D_y + D_z). \quad (12)$$

The good agreement (within the range of fluctuations) of the final D values calculated for 298 K using the Eqs. (8)–(11) (as shown in Fig. 1), indicates that the diffusion time used in the evaluation procedure exceeds the correlation time. The self-diffusion coefficients calculated in this way at 298 and 393 K are summarized in Table 1.

It can be seen from these results that the largest component of the diffusion tensor is D_y . The D_y values are about two times larger than D_x at both temperatures and about seven times larger than D_z at 298 K and even larger at 393 K. This is consistent with the physical structure of the silicalite-1 crystal, which consists of zigzag channels lying in the xz -plane and the straight channels lying parallel to the y -axis. This causes the

Table 1

The diffusion coefficients D_x , D_y and D_z , of water molecules in x -, y - and z -directions as well as the average value D (one-third of the trace of the diffusion tensor) obtained from the simulations and comparison with the mean diffusivity obtained in the PFG NMR studies at 298 and 393 K

Temperature (K)	MD simulation				PFG NMR D ($\text{m}^2 \text{s}^{-1}$)
	D_x ($\text{m}^2 \text{s}^{-1}$)	D_y ($\text{m}^2 \text{s}^{-1}$)	D_z ($\text{m}^2 \text{s}^{-1}$)	D ($\text{m}^2 \text{s}^{-1}$)	
298	2.6×10^{-9}	6.5×10^{-9}	7.9×10^{-10}	3.3×10^{-9}	1.7×10^{-9}
393	5.7×10^{-9}	1.3×10^{-8}	1.4×10^{-9}	6.7×10^{-9}	1.5×10^{-9}

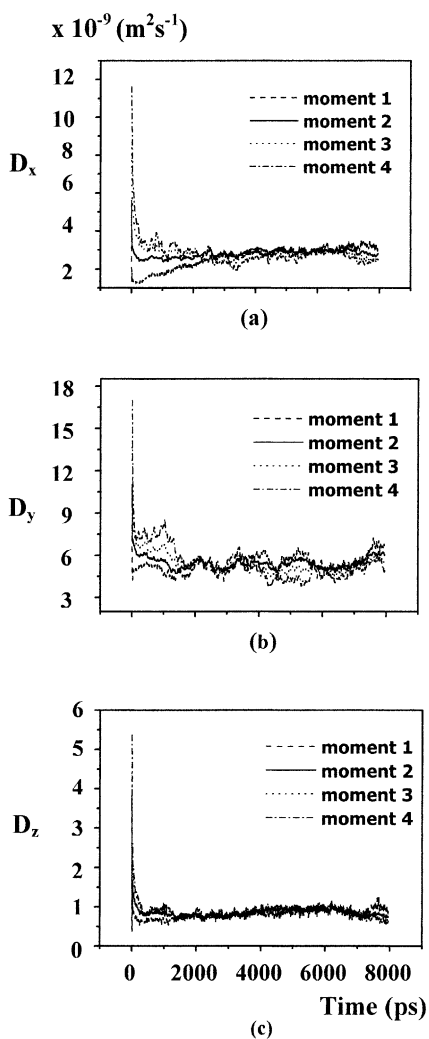


Fig. 1. The diffusion coefficients in (a) x -axis; (b) y -axis; (c) z -axis vs. time window (0.4 ns) obtained from the simulations with two water molecules per intersection of silicalite-1 at 298 K.

significant difference of the elementary diffusion rates in different directions.

Considering the diffusion through silicalite-1 as a random walk of independent steps between the channel intersections, the main elements of the diffusion tensor may be shown to be correlated by the relation [23]:

$$\frac{c^2}{D_z} = \frac{a^2}{D_x} + \frac{b^2}{D_y}, \quad (13)$$

where a , b and c are the unit cell lengths. Eq. (13) implies that the correlation time of propagation is shorter than the mean time it takes a molecule to travel from intersection to intersection. Possible deviations from this case, i.e. correlated motion between the channel intersections, may be accounted for by introducing a parameter [24–26]:

$$\beta = \frac{c^2/D_z}{a^2/D_x + b^2/D_y} \quad (14)$$

The case $\beta = 1$, obviously represents the above considered case of completely random steps. The case $\beta > 1$ indicates preferential continuation of the diffusion path along one and the same channel, while $\beta < 1$ stands for molecular propagation with interchanges between the two channel types more probable than at random. The values of β calculated in this study are equal to 1.04 at 298 K and 1.25 at 393 K. In agreement with the behavior found for alkanes, e.g. [26], where $\beta = 1.2$ and 1.3, a tendency is observed that the xenon molecules and the methane molecules, respectively, in silicalite-1 prefer to remain in the same type rather than to change into a segment of the other channel type at a channel intersection.

The oxygen–oxygen radial distribution functions g for the water molecules at the two temperatures have been calculated and displayed in Fig. 2. In inhomogeneous systems, $g(r_1, r_2)$ depends upon r_1 , also, and is not simply $g(r)$ with $r = |r_1 - r_2|$. But, as a first approximation, we have done the evaluation of $g(r)$ like in a homogeneous isotropic system. This is equivalent to an averaging over the sites r_1 taking as a weight

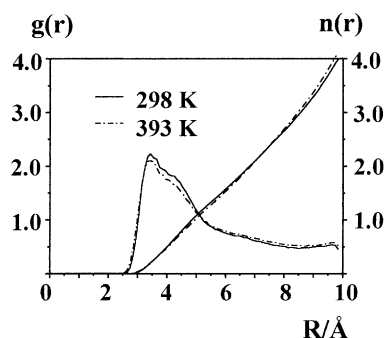


Fig. 2. Oxygen–oxygen radial distribution functions and corresponding running integration numbers for water molecules obtained from the simulations at 298 and 393 K.

function the relative number of events when the r_1 are found during the MD run. Note that due to the asymmetry of the silicalite-1 lattice the function $g(r)$, defined in this way, does not converge to 1.0 for distances of the order of 10 Å. The function $g(r) = 1$ would correspond to a homogeneous distribution in space that can be observed in systems with a structure on molecular level only at a length scale that is larger than the size of the inhomogeneities, i.e. the channel structure in the present case. The radial density distributions show a first maximum at 3.5 Å followed by a pronounced shoulder centered at 4.4 Å. In order to see the number of neighbors the integral $n(r)$ of $g(r)$ is also displayed in Fig. 2. It can be seen that, e.g. within a distance of 7 Å around a given water molecule, there are in average only two other water molecules.

To decide whether the water molecules form clusters, the distribution of coordination numbers is examined. As the first minimum is not well-defined, the probability $P_r(i)$ to find 1, 2, 3, ... water molecules within $r = 4, 5$ and 6 Å around a given one was examined for both temperatures and compared in Fig. 3. The highest probability is found for the number zero of water molecules in all cases. The average coordination numbers at 298 K integrated up to the three distances are 0.36, 0.94 and 1.44, respectively. The corresponding numbers at 393 K are 0.36, 0.90 and 1.40. It can be concluded that the simulations did not show any clustering of water molecules in the silicalite-1 channels for the examined temperatures and concentrations of guest molecules.

3. PFG NMR measurements

3.1. Experimental details

The measurements of self-diffusion of guest molecules in samples of silicalite-1 were carried out using the home-built PFG NMR spectrometer FE-GRIS 400 operating at a ^1H resonance frequency of 400 MHz [17]. For diffusion measurements, the standard stimulated echo and Hahn echo PFG NMR pulse sequences [18] were used. To obtain the diffusivity, the attenuation of the PFG NMR spin echo signal (Ψ) was measured as a function of the amplitude of the applied field gradient (g). For the PFG NMR diffusion measurements using both sequences the duration of the applied field gradient pulses (δ)

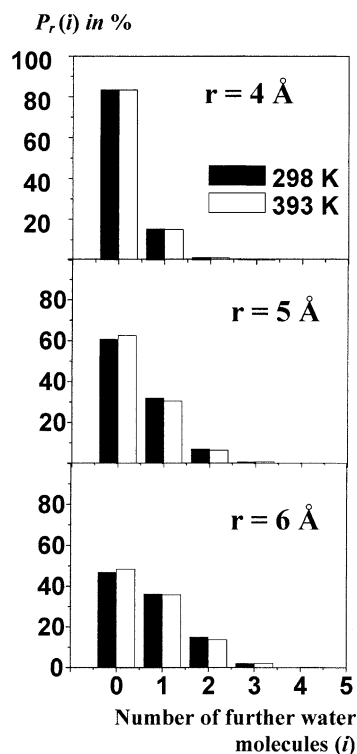


Fig. 3. Representation of nearest-neighbor probabilities: the heights of the columns represent the probability $P_r(i)$ to find i further water molecules within a distance of r (4, 5 and 6 Å) around a given water molecule. Distance means the distance between the oxygen atoms in the water molecules.

was set to 0.26 ms and the duration of the ‘dephasing’ and the ‘read’ intervals (τ) was set to 0.8 ms. For the PFG NMR measurements using the stimulated echo sequence the value of the time interval between the two gradient pulses (Δ) was in the range between 1.2 and 2 ms. The intensity of the applied gradients was varied between 0 and 24 T m $^{-1}$.

The average size of silicalite-1 crystals was 100 $\mu\text{m} \times 30 \mu\text{m} \times 20 \mu\text{m}$. The zeolite was used in the calcined form. The sample of silicalite-1, applied in the PFG NMR studies was synthesized as described in [19]. The investigations of this sample using H^1 MAS NMR revealed the presence of silanol groups (around one silanol group per two unit cells).

The samples for the PFG NMR measurements were prepared with the following method. Around 300 mg of silicalite-1 were introduced into the NMR tube. Then the tube was connected to the vacuum system

and the zeolite sample was activated by keeping the sample under high vacuum at 473 K for 20 h. Subsequently, the zeolite sample was loaded with water by freezing it from a fixed volume of the vacuum system. When preparing the samples with D₂O–alkane mixtures, upon loading with D₂O the samples were additionally loaded with alkane by freezing it from another fixed volume of the vacuum system. Upon loading, the NMR tube was sealed and separated from the vacuum system. The total amounts adsorbed corresponded to 24 mg g⁻¹ of water in the alkane-free sample and to 28 mg g⁻¹ of D₂O in the samples with the D₂O–alkane mixtures. These are exactly the concentrations considered in the MD simulations. The amounts of ethane, propane and *n*-butane adsorbed in the samples with the D₂O–alkane mixtures as well as in the samples loaded only with alkane were 42, 61 and 81 mg g⁻¹, respectively.

3.2. Results of the pulsed field gradient nuclear magnetic resonance measurements

Fig. 4 shows examples of the attenuation of the NMR signal ($\Psi(g, \Delta) \equiv \frac{M(g, \Delta)}{M(0, \Delta)}$) of water molecules in the sample of silicalite-1 at 298 and 393 K. The attenuation curves were recorded using

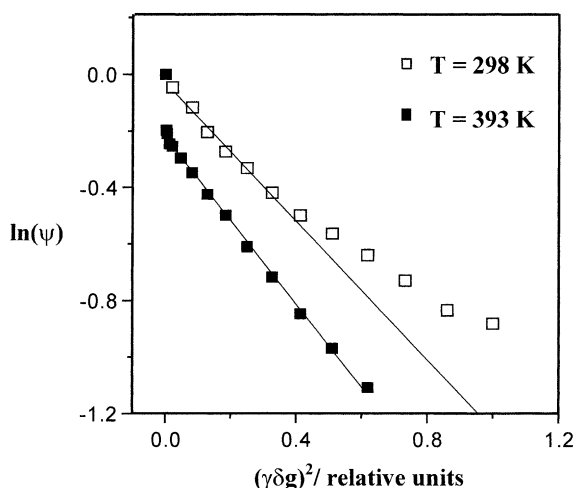


Fig. 4. ¹H PFG NMR spin echo attenuation curves for water in the sample of silicalite-1 recorded by using the stimulated echo PFG NMR sequence at 298 K ($\Delta = 2$ ms) and by using the Hahn echo PFG MR sequence at 393 K ($\Delta = 0.8$ ms). The lines show the fit curves used to calculate the diffusion coefficients.

the stimulated echo and the Hahn echo PFG NMR sequences. For both sequences the spin echo attenuation can be written as [21]:

$$\Psi(g, \Delta) = \exp\left(-\gamma^2 D \delta^2 g^2 \left(\Delta - \frac{1}{3}\delta\right)\right), \quad (15)$$

where γ and D denote the gyromagnetic ratio and the diffusion coefficient. In deriving Eq. (15) it was assumed, that the diffusion can be described by a normal Gaussian propagator, given in Eq. (3), which represents the probability density for the diffusing molecules to be displaced over a distance $|\mathbf{r} - \mathbf{r}_0|$ during a time interval t . It was shown in [27] that for sufficiently small PFG NMR attenuations measured in powder samples, Eq. (15) is a good approximation even for anisotropic diffusion like diffusion in silicalite-1.

This diffusivity can be obtained from the initial slope of the $\ln(\Psi)$ versus g^2 representation using Eq. (15). For sufficiently large PFG NMR attenuations diffusion anisotropy leads to deviations from the linear dependence of $\ln(\Psi)$ on g^2 as predicted by Eq. (15).

It is seen in Fig. 4 that the attenuation curve measured at 298 K shows a pronounced non-linear behavior. At the same time, the curve measured at 393 K exhibits only minor deviations from a linear behavior except for the very rapid decay in the initial part of the curve. The deviations of the attenuation curves in Fig. 4 from straight lines can be attributed to the diffusion anisotropy of water molecules in silicalite-1 and/or to the existence of the distribution of the diffusivities of water molecules in silicalite-1 samples. Note that the root mean square displacements of water molecules were always sufficiently small in comparison to the size of the crystals so that the effect of diffusion restriction of water molecules in the crystals by the outer surface of the crystals was negligible. Hence, it is unlikely that the diffusion restriction is the reason of the deviations of the measured attenuation curves from the linear dependencies predicted by Eq. (15). An existence of a distribution of the diffusivities of the water molecules in the silicalite-1 samples, on the other hand, is feasible. It can be assumed that a part of the water molecules in the sample forms monolayers on the external surfaces of the zeolite crystals or even exists in the form of the liquid. The difference between the diffusion coefficient of this type of water and that of water molecules residing in silicalite-1 crystals can

lead to the non-linear attenuation curves at 298 K. The diffusivity obtained from the initial slope of the attenuation curve measured at 298 K (Fig. 4) is equal to $1.7 \times 10^2 \text{ m}^2 \text{ s}^{-1}$. This diffusivity can be attributed to the characteristic, mean diffusivity of all the types of water in the sample. A heating of the sample up to 393 K will reduce or completely eliminate the liquid phase and the monolayers of water in the sample. At this temperature the water molecules can be expected either to be primarily in the gas phase of the NMR sample or to reside in silicalite-1 crystals. This is in agreement with the experimental observation of the very fast initial signal decay followed by the almost linear signal decay at 393 K (Fig. 4). The fast initial decay can be attributed primarily to the water in the gas phase while the slower portion of the attenuation curve can be assigned to the water in silicalite-1 crystals. The diffusion coefficient of water obtained from the slower portion of the attenuation curve (Fig. 4) using Eq. (15) is equal to $1.5 \times 10^{-9} \text{ m}^2 \text{ s}^{-1}$. This diffusivity is significantly lower than the diffusivity of water in the liquid phase even at 373 K ($8.7 \times 10^{-9} \text{ m}^2 \text{ s}^{-1}$ from [28]). Hence, the diffusivity measured at 393 K may definitely not be assigned to the diffusion coefficient of water in a liquid or a quasi-liquid phase. We tentatively assign this diffusivity to the diffusion of water in silicalite-1 crystals. The small deviations of the slower part of the attenuation curve from a straight line (Fig. 4, at 393 K) may be attributed primarily to the diffusion anisotropy in silicalite-1 crystals.

The study of the diffusion of one component in zeolite under the influence of other diffusants was recently a point of interest for both theoreticians and experimentalists [26,29–31]. It was generally observed that the diffusivity of one component kept at a constant loading decreases as the loading level of another, usually less mobile component increases. Here, we report the preliminary results of the PFG NMR diffusion measurements of ethane, propane and *n*-butane in samples of silicalite-1 with and without pre-adsorbed D₂O. The loadings of alkanes in both types of the samples were kept at the same level. In all cases the initial part of the PFG NMR attenuation curves ($-1.0 < \ln(\Psi) < 0.0$) of alkane diffusion in silicalite-1 shows the linear behavior as predicted by Eq. (15). The diffusion coefficients of the alkanes in the samples with and without water are presented in Table 2. The diffusivities were obtained from the

Table 2

The diffusion coefficients *D* of ethane, propane and *n*-butane obtained from the PFG NMR measurements at 298 K in the samples of silicalite-1 with and without pre-adsorbed D₂O

Alkane	<i>D</i> without pre-adsorbed D ₂ O (m ² s ⁻¹)	<i>D</i> with pre-adsorbed D ₂ O (m ² s ⁻¹)
Ethane	1.3×10^{-9}	4.0×10^{-10}
Propane	4.4×10^{-10}	2.2×10^{-10}
<i>n</i> -Butane	1.9×10^{-10}	1.4×10^{-10}

initial slope of the attenuation curves. Diffusion studies of small alkanes in water-free MFI-type zeolites by the PFG NMR technique are reported in [29,32–34]. The comparison of the present data obtained for the water-free samples with those previously reported shows general agreement between the absolute values of the diffusion coefficients. The data presented in Table 2 show that the diffusivities of all three alkanes are lower in the samples with pre-adsorbed water than in the water-free samples. It can be seen in Table 2 that for smaller, more mobile alkanes the influence of water on the self-diffusion of alkane molecules is larger. This observation is in qualitative agreement with the results previously reported for other two-component systems [26,29–31]. The data presented in Table 2 provide, in our opinion, evidence that under our experimental conditions significant loadings of water molecules in silicalite-1 crystals are achieved.

4. Comparison and conclusions

MD simulations carried out at 298 and 393 K at a concentration of two water molecules per intersection using an ab initio fitted potential model that has been obtained from ab initio calculations do not show cluster formation of water in silicalite-1. So, diffusion coefficients that agree with experimental values could be expected.

The PFG NMR results reported in this paper indicate that under our experimental conditions not only extra-crystalline but also intra-crystalline water is present in the silicalite-1 samples. This conclusion is supported by the observation of the influence of pre-adsorbed water on the intra-crystalline diffusivities of alkane molecules in silicalite-1 as well as by the comparison of the measured diffusivity of water in silicalite-1 sample at 393 K with that of liquid water.

Although our PFG NMR results are preliminary in nature they allow us to estimate the intra-crystalline diffusivity of water at 393 K. This value differs by less than one order of magnitude from the results of MD simulations at the same temperature. In view of the fact that for other zeolitic adsorbate–adsorbent systems like, e.g. longer alkanes in MFT, there are still orders-of-magnitude differences between experimental results and MD simulations (see e.g. [35]), this first comparative study of MD simulation and measurement of water diffusion in zeolites appears to yield reasonable agreement.

Acknowledgements

Computing facilities provided by the Austrian-Thai Center for Chemical Education and Research at Chulalongkorn University, the National Electronic and Computer Technology Center, Bangkok, Thailand are gratefully acknowledged. The authors acknowledge support by the Thailand Research Fund (PHD/0090/2541), Deutscher Akademischer Austauschdienst (A/99/16872) the Deutsche Forschungsgemeinschaft (SFB294) and the Fonds der chemischen Industrie. We thank Prof. Dr. Helmut Papp, Leipzig and Dr. Eckhard Spohr, Jülich, for useful discussions, and Dr. David Ruffolo, Bangkok, for proofreading the manuscript.

References

- [1] M. Anpo, S. Guo Zhang, S. Higashimoto, M. Matsuoka, H. Yamashita, Y. Ichihashi, Y. Matsumura, Y. Souma, *J. Phys. Chem. B* 103 (1999) 9295.
- [2] K. Kageyama, S. Ogino, T. Aida, T. Tatsumi, *Macromolecules* 31 (1998) 4069.
- [3] C.N.R. Rao, S. Natarajan, S. Neeraj, *J. Am. Chem. Soc.* 122 (2000) 2810.
- [4] E. Jolimaître, M. Tayakout-Fayolle, C. Jallut, K. Ragil, *Ind. Eng. Chem. Res.* 40 (2001) 914.
- [5] T. Sano, S. Ejiri, K. Yamada, Y. Kawakami, H. Yanagishita, *J. Membr. Sci.* 123 (1997) 225.
- [6] T. Sano, M. Hasegawa, Y. Kawakami, H. Yanagishita, *J. Membr. Sci.* 107 (1995) 193.
- [7] J. Caro, S. Hocevar, J. Kärger, L. Riekert, *Zeolites* 6 (1986) 213.
- [8] V.V. Turov, V.V. Brei, K.N. Khomeenko, R. Leboda, *Micropor. Mesopor. Mater.* 23 (1998) 189; P.H. Kasai, P.M. Jones, *J. Mol. Cat.* 27 (1983) 81.
- [9] M.P. Allen, D.J. Tildesley, *Computer Simulation of Liquids*, Clarendon Press, Oxford, 1990.
- [10] R. Haberlandt, S. Fritzsche, G. Peinel, K. Heinzinger, *Molekulardynamik: Grundlagen und Anwendungen*, Vieweg, Göttingen, 1995.
- [11] D.H. Olson, G.T. Kokotailo, S.L. Lawton, W.M. Meier, *J. Phys. Chem.* 85 (1981) 2238.
- [12] P. Bopp, G. Jancso, K. Heinzinger, *Chem. Phys. Lett.* 98 (1983) 129.
- [13] C. Bussai, S. Hannongbua, S. Fritzsche, R. Haberlandt, Ab initio potential energy surface and MD simulations for the determination of the diffusion coefficient of water in silicalite, *Chem. Phys. Lett.* B 105 (2001) 3409.
- [14] S. Fritzsche, M. Wolfsberg, R. Haberlandt, *Chem. Phys.*, submitted for publication.
- [15] H. Dufner, S.M. Kast, J. Brickmann, M. Schlenkrich, *J. Comp. Chem.* 18 (1997) 660.
- [16] D. Wolf, P. Keblinski, S.R. Phillpot, J. Eggebrecht, *J. Chem. Phys.* 110 (1999) 17.
- [17] J. Kärger, N.-K. Bär, W. Heink, H. Pfeifer, G. Seiffert, *Z. Naturforsch Teil A* 50 (1996) 186.
- [18] J. Kärger, D.M. Ruthven, *Diffusion in Zeolites and Other Microporous Solids*, Wiley, New York, 1992.
- [19] B. Staudte, A. Gutsze, W. Böhlmann, H. Pfeifer, B. Pietrewicz, *Micropor. Mesopor. Mater.* 40 (2000) 1.
- [20] S. Fritzsche, R. Haberlandt, J. Kärger, H. Pfeifer, K. Heinzinger, *Chem. Phys. Lett.* 198 (1992) 283.
- [21] J. Kärger, H. Pfeifer, W. Heink, Principles and application of self-diffusion measurements by nuclear magnetic resonance, in: *Advances in Magnetic Resonance*, Vol. 12, Academic Press, New York, 1988.
- [22] R. Haberlandt, J. Kärger, *Chem. Eng. J.* 74 (1999) 15.
- [23] J. Kärger, *J. Phys. Chem.* 98 (1991) 5558.
- [24] E.J. Maginn, A.T. Bell, D.N. Theodorou, *J. Phys. Chem.* 100 (1996) 7155.
- [25] J. Kärger, P. Demontis, G.B. Suffritti, A. Tilocca, *J. Chem. Phys.* 110 (1999) 2.
- [26] S. Jost, N.K. Bär, S. Fritzsche, R. Haberlandt, J. Kärger, *J. Phys. Chem. B* 102 (1998) 6375.
- [27] U. Hong, J. Kärger, R. Kramer, H. Pfeifer, G. Seiffert, U. Müller, K.K. Unger, H.-B. Lück, T. Ito, *Zeolites* 11 (1991) 816; U. Hong, J. Kärger, H. Pfeifer, U. Müller, K.K. Unger, *Z. Phys. Chem. (Leipzig)* 173 (1991) 225.
- [28] K. Holz, S.R. Heil, A. Sacco, *Phys. Chem. Chem. Phys.* 2 (2000) 4740.
- [29] R.Q. Snurr, J. Kärger, *J. Phys. Chem. B* 101 (1997) 6469.
- [30] S. Jost, N.K. Bär, S. Fritzsche, R. Haberlandt, *Chem. Phys. Lett.* 219 (1997) 385.
- [31] L.N. Gergidis, D.N. Theodorou, H. Jobic, *J. Phys. Chem. B* 104 (2000) 5541.
- [32] J. Caro, M. Bülow, W. Schirmer, J. Kärger, W. Heink, H. Pfeifer, *J. Chem. Soc. Faraday Trans. I* 81 (1985) 2541.
- [33] W. Heink, J. Kärger, H. Pfeifer, K.P. Datema, A.K. Nowak, *J. Chem. Soc. Faraday Trans.* 88 (1992) 3505.
- [34] W.D. Ylstra, H.P.C.E. Kuipers, M.F.M. Post, J. Kärger, *J. Chem. Soc. Faraday Trans.* 87 (1991) 1935.
- [35] H. Jobic, *Recent Advances in Gas Separation by Microporous Ceramic Membranes*, Elsevier, Amsterdam, 2000.